

A Theoretical Framework for Data Efficient Multi-Source Transfer Learning Based on Cramér-Rao Bound

Qingyue Zhang^{*1} Haohao Fu^{*1} Guanbo Huang^{*1} Yaoyuan Liang¹ Chang Chu¹ Tianren Peng¹ Yanru Wu¹
 Qi Li¹ Yang Li¹ Shao-Lun Huang¹

Abstract

Multi-source transfer learning provides an effective solution to data scarcity in real-world supervised learning scenarios by leveraging multiple source tasks. In this field, existing works typically use all available samples from sources in training, which constrains their training efficiency and may lead to suboptimal results. To address this, we propose a theoretical framework that answers the question: what is the optimal quantity of source samples needed from each source task to jointly train the target model? Specifically, we introduce a generalization error measure that aligns with cross-entropy loss, and minimize it based on the Cramér-Rao Bound to determine the optimal transfer quantity for each source task. Additionally, we develop an architecture-agnostic and data-efficient algorithm OTQMS to implement our theoretical results for training deep multi-source transfer learning models. Experimental studies on diverse architectures and two real-world benchmark datasets show that our proposed algorithm significantly outperforms state-of-the-art approaches in both accuracy and data efficiency. The code and supplementary materials are available in <https://anonymous.4open.science/r/Materials>.

1. Introduction

Nowadays, various machine learning algorithms have achieved remarkable success by leveraging large-scale labeled training data. However, in many practical scenarios, the limited availability of labeled data presents a significant challenge, where transfer learning emerges as an effective solution (Zhao et al., 2020). Transfer learning aims

^{*}Equal contribution ¹Tsinghua Shenzhen International Graduate School, Tsinghua University, Shenzhen, China. Correspondence to: Shao-Lun Huang <twn2gold@gmail.com>, Yang Li <yangli@sz.tsinghua.edu.cn>.

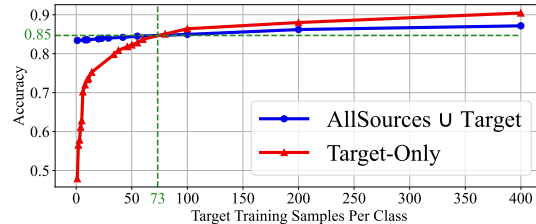


Figure 1: **More source samples does not always mean better performance.** Incorporating all source samples may bring negative impact, which is illustrated by the comparison of two strategies, using target with all source samples (blue) and using target only (red), evaluated on the equally divided 5-task CIFAR10 dataset. Theoretically, although incorporating more source samples reduces model variance by expanding the training data, the discrepancy between the source and target tasks introduces additional bias.

to leverage knowledge from tasks with abundant data or being well-trained, known as the source tasks, to improve the performance of a new learning task, known as the target task. Given its numerous applications, transfer learning has gained wide popularity and seen success in a variety of fields, such as computer vision (Wang & Deng, 2018), natural language processing (Sung et al., 2022), recommendation system (Fu et al., 2024) and anomaly detection (Vincent et al., 2020). Traditionally, transfer learning has focused on the transfer between a single source task and a target task. However, there is a growing emphasis on multi-source transfer learning, which leverages multiple source tasks to enhance the training of the target task (Sun et al., 2015).

In multi-source transfer learning, traditional methods usually jointly train the target model using all available samples from sources without selection (Zhang et al., 2024; Shui et al., 2021; Li et al., 2021b). This evidently poses a severe limitation to training efficiency, considering the vast number of available samples from various potential source tasks in real-world scenarios (Peng et al., 2019). Moreover, directly assuming the use of all available samples seriously constrains their solution space, which possibly leads to suboptimal results as illustrated in Figure 1. Therefore, it is critical to establish a theoretical framework to answer the question: *what is the optimal transfer quantity of source*

Table 1: **Comparison across matching-based transfer learning method**, based on whether they are tailored to multi-sources, have task generality, have shot generality, and require target labels. The ‘✓’ represents obtaining the corresponding aspects, while ‘✗’ the opposite. Task generality denotes the ability to handle various target task types, and shot generality denotes the ability to avoid negative transfer in different target sample quantity settings including few-shot and non-few-shot.

Method	Multi-Source	Task Generality	Shot Generality	Target Label
MCW (Lee et al., 2019)	✓	✗	✗	Supervised
Leep (Nguyen et al., 2020)	✗	✓	✓	Supervised
Tong (Tong et al., 2021)	✓	✗	✓	Supervised
DATE (Han et al., 2023)	✓	✓	✓	Unsupervised
H-ensemble (Wu et al., 2024)	✓	✗	✗	Supervised
OTQMS (Ours)	✓	✓	✓	Supervised

samples from each source task needed in training the target task?

In this work, we establish a theoretical framework for the multi-source transfer learning problem. We formulate the transfer quantity of each source task as an optimization variable and propose a method to determine its optimal value. Specifically, we introduce the expectation of Kullback-Leibler (K-L) divergence between the distribution learned from training samples and the true distribution of target task samples as a measure of generalization error. This measure is then minimized based on the Cramér-Rao Bound to derive the optimal transfer quantity of each source task. Building on this, we propose a practical algorithm, named **Optimal Transfer Quantities for Multi-Source Transfer learning (OTQMS)**, to implement our theoretical results for training deep multi-source transfer learning models. Notably, OTQMS is data-efficient and compatible with various model architectures, including Vision Transformer (ViT) and Low-Rank Adaptation (LoRA). It also demonstrates advantages in *task generality* and *shot generality* (as illustrated in Table 1), since we establish our theoretical framework without restricting it to a specific target task type or limiting the range of target sample quantity.

In summary, our main contributions are as follows:

- a) A novel theoretical framework that optimizes transfer quantities is introduced for multi-source transfer learning. We propose a new K-L divergence measure of the generalization error. By minimizing it, we develop a method to determine the optimal transfer quantity of each source task.
- b) Based on the framework, we propose OTQMS, an architecture-agnostic and data-efficient algorithm for target model training in multi-source transfer learning.
- c) Experimental studies on two real-world datasets and various model architectures demonstrate that OTQMS achieves significant improvements in both accuracy

and data efficiency. In terms of accuracy, OTQMS outperforms state-of-the-art by an average of 1.5% on DomainNet and 1.0% on Office-Home. In terms of data efficiency, OTQMS reduces the average training time by 35.19% and the average sample usage by 47.85% on DomainNet. Furthermore, extensive supplementary experiments demonstrate that our theory can facilitate both full model training and parameter-efficient training.

2. Related Work

2.1. Transfer Learning Theory

Existing theoretical works can be categorized into two groups. The first group focuses on proposing measures to quantify the similarity between the target and source tasks. Within this group, some measures have been introduced, including l_2 -distance (Long et al., 2014), optimal transport cost (Courty et al., 2016), LEEP (Nguyen et al., 2020), Wasserstein distance (Shui et al., 2021), and maximal correlations (Lee et al., 2019). This work belongs to the second group focusing on developing new generalization error measures. Within this group, the measures having been introduced include f -divergence (Harremoës & Vajda, 2011), mutual information (Bu et al., 2020), χ^2 -divergence (Tong et al., 2021), \mathcal{H} -score (Bao et al., 2019; Wu et al., 2024). However, the potential of K-L divergence as a generalization error measure has not been sufficiently explored.

2.2. Multi-source Transfer Learning

Classified by the object of transfer, existing multi-source transfer learning methods mainly focus on two types: model transfer vs sample transfer (Zhuang et al., 2020). Model transfer assumes there is one or more pre-trained models on the source tasks and transfers their parameters to the target task via fine-tuning (Wan et al., 2022). This work focuses on the latter, which is based on joint training of the source task samples with those of the target task (Zhang

et al., 2024; Shui et al., 2021; Li et al., 2021b). Classified by the strategy of transfer, existing methods mainly focus on two types: alignment strategy and matching-based strategy (Zhao et al., 2024). Alignment strategy aims to reduce the domain shift among source and target domains (Li et al., 2021a; Zhao et al., 2021; Li et al., 2021b). This work is more similar to the latter, focusing on determining which source domains or samples should be selected or assigned higher weights for transfer (Guo et al., 2020; Shui et al., 2021; Tong et al., 2021; Wu et al., 2024). However, most existing works either utilize all samples from all sources or perform task-level selection, whereas this work explores a framework that optimizes the transfer quantity of each source task.

3. Problem Formulation

Consider the transfer learning setting with one target task \mathcal{T} , and K source tasks $\{\mathcal{S}_1, \dots, \mathcal{S}_K\}$. The target task \mathcal{T} is not restricted to a specific downstream task category. Generally, we formulate it as a parameter estimation problem under a distribution model $P_{X;\underline{\theta}}$. For example, when \mathcal{T} is a supervised classification task, $P_{X;\underline{\theta}}$ corresponds to the joint distribution model of input features Z and output labels Y , i.e., $X = (Z, Y)$. Our objective is to estimate the true value of $\underline{\theta}$, which corresponds to optimizing the neural network parameters for target task \mathcal{T} . Here, θ denotes 1-dimensional parameter, and $\underline{\theta}$ denotes high dimensional parameter.

Furthermore, we assume that the source tasks and the target task follow the same parametric model and share the same input space \mathcal{X} . Without loss of generality, we assume \mathcal{X} to be discrete, though our results can be readily extended to continuous spaces. The target task \mathcal{T} has N_0 training samples $X^{N_0} = \{x_1, \dots, x_{N_0}\}$ i.i.d. generated from some underlying joint distribution $P_{X;\underline{\theta}_0}$, where the parameter $\underline{\theta}_0 \in \mathbb{R}^d$. Similarly, the source task \mathcal{S}_k has N_k training samples $X^{N_k} = \{x_1^k, \dots, x_{N_k}^k\}$ i.i.d. generated from some underlying joint distribution $P_{X;\underline{\theta}_k}$, where $k \in [1, K]$, and the parameter $\underline{\theta}_k \in \mathbb{R}^d$. In this work, we use the Maximum Likelihood Estimator (MLE) to estimate the true target task parameter $\underline{\theta}_0$. Moreover, the following lemma demonstrates that, for large sample size, the MLE can achieve the theoretical lower bound of the Mean Squared Error (MSE) asymptotically, known as the Cramér-Rao Bound.

Lemma 3.1. (Cover & Thomas, 2006) *Let $\hat{\underline{\theta}}$ be an unbiased estimator of $\underline{\theta}_0$ based on n i.i.d. samples. Then, the MSE matrix of $\hat{\underline{\theta}}$ satisfies the following lower bound:*

$$MSE(\hat{\underline{\theta}})^{d \times d} \triangleq \mathbb{E} \left[\left(\hat{\underline{\theta}} - \underline{\theta}_0 \right) \left(\hat{\underline{\theta}} - \underline{\theta}_0 \right)^T \right] \geq \frac{1}{n} J(\underline{\theta}_0)^{-1}, \quad (1)$$

where $\left(\hat{\underline{\theta}} - \underline{\theta}_0 \right)$ is d -dimensional vector, and the matrix

inequality $A \geq B$ means that $A - B$ is positive semi-definite. In addition, the $J(\underline{\theta})$ is fisher information matrix defined as:

$$J(\underline{\theta})^{d \times d} = \mathbb{E} \left[\left(\frac{\partial}{\partial \underline{\theta}} \log P(X; \underline{\theta}) \right) \left(\frac{\partial}{\partial \underline{\theta}} \log P(X; \underline{\theta}) \right)^T \right]. \quad (2)$$

Moreover, as the sample size $n \rightarrow \infty$, the MLE $\hat{\underline{\theta}}$ can achieve this bound asymptotically, i.e.,

$$MSE(\hat{\underline{\theta}}) = \frac{1}{n} J(\underline{\theta}_0)^{-1} + o\left(\frac{1}{n}\right). \quad (3)$$

It should be noted that in some works, the MSE is defined as a scalar, which corresponds to the trace of the MSE matrix and can also be bounded using this lemma.

When we transfer n_1, \dots, n_K samples from the $\{\mathcal{S}_1, \dots, \mathcal{S}_K\}$, where $n_k \in [0, N_k]$, we denote these training sample sequences as $X^{n_1}, X^{n_2}, \dots, X^{n_K}$. Then, the MLE for multi-source transfer learning, in the simplest form, is a summation of the likelihood of all source tasks and target tasks, i.e.,

$$\hat{\underline{\theta}} = \arg \max_{\underline{\theta}} \sum_{x \in X^{N_0}} \log P_{X;\underline{\theta}}(x) + \sum_{k=1}^K \sum_{x \in X^{n_k}} \log P_{X;\underline{\theta}}(x). \quad (4)$$

In this work, our goal is to derive the optimal transfer quantities n_1^*, \dots, n_K^* of source tasks $\mathcal{S}_1, \dots, \mathcal{S}_K$ to minimize certain divergence measure \mathcal{L} between the distribution learned from training samples $P_{X;\hat{\underline{\theta}}}$ and the true distribution of target task $P_{X;\underline{\theta}_0}$, i.e.,

$$n_1^*, \dots, n_K^* = \arg \min_{n_1, \dots, n_K} \mathcal{L}(P_{X;\hat{\underline{\theta}}}, P_{X;\underline{\theta}_0}). \quad (5)$$

Besides, we provide the notations table in Appendix A.

4. Theoretical Analysis and Algorithm

In this section, we will first introduce a new K-L divergence measure for the optimization problem in (5). Then, we will analyze it based on the Cramér-Rao bound to derive the optimal transfer quantities for both single-source and multi-source scenarios. Finally, we will develop a practical algorithm based on the theoretical framework.

Definition 4.1. (The K-L divergence) The K-L divergence measures the difference between two probability distributions $P(X)$ and $Q(X)$ over the same probability space. It is defined as:

$$D(P||Q) = \sum_{x \in \mathcal{X}} p(x) \log \frac{p(x)}{q(x)}.$$

In this work, we apply the K-L divergence between the distribution model parameterized by MLE (4) and the true distribution model of target task to measure the generalization error, which directly corresponds to the testing error using cross-entropy loss (Cover & Thomas, 2006).

$$D\left(P_{X;\hat{\theta}} \parallel P_{X;\theta_0}\right) = \underbrace{-H(P_{X;\hat{\theta}})}_{\text{entropy}} + \underbrace{\mathbb{E}_{P_{X;\hat{\theta}}}[P_{X;\theta_0}]}_{\text{cross-entropy}}.$$

Finally, our generalization error measure is defined as follows.

$$\mathcal{L}(P_{X;\hat{\theta}}, P_{X;\theta_0}) = \mathbb{E}\left[D\left(P_{X;\hat{\theta}} \parallel P_{X;\theta_0}\right)\right]. \quad (6)$$

4.1. Single-Source Transfer Learning

The direct computation of the proposed K-L divergence measure is challenging. Fortunately, we can prove that the proposed K-L measure directly depends on the MSE in the asymptotic case. Moreover, the MSE has a widely used Cramér-Rao bound introduced in Lemma 3.1, which provides a bound on the estimator’s error, and is asymptotically tight. As our goal is to find a correspondence between transfer quantity and generalization error, for the rest of the paper, we mainly analyze the K-L measure based on the Cramér-Rao bound (3). To begin, we consider the setting with a target task \mathcal{T} with N_0 samples generated from a model with 1-dimensional parameter.

Lemma 4.2. (proved in Appendix B.1) *Given a target task \mathcal{T} with N_0 i.i.d. samples generated from 1-dimensional underlying model $P_{X;\theta_0}$, where $\theta_0 \in \mathbb{R}$, and denoting $\hat{\theta}$ as the MLE (4) based on the N_0 samples, then the K-L measure (6) can be expressed as:*

$$\mathbb{E}\left[D\left(P_{X;\hat{\theta}} \parallel P_{X;\theta_0}\right)\right] = \frac{1}{2N_0} + o\left(\frac{1}{N_0}\right). \quad (7)$$

The result of Lemma 4.2 demonstrates that when there is only a target task, our K-L measure is inversely proportional to the number of training samples. Next, we consider the transfer learning scenario in which we have one target task \mathcal{T} with N_0 training samples and one source task \mathcal{S}_1 with N_1 training samples. In this case, We aim to determine the optimal transfer quantity $n_1^* \in [1, N_1]$. To facilitate our mathematical derivations, we assume N_0 and N_1 are asymptotically comparable, and the distance between the parameters of target task and source task is sufficiently small (i.e., $|\theta_0 - \theta_1| = O(\frac{1}{\sqrt{N_0}})$). Considering the similarity of low-level features among tasks of the same type, this assumption is made without loss of generality. Furthermore, as demonstrated in subsequent analysis, our conclusions remain valid even in extreme cases where the distance between parameters is large.

Theorem 4.3. (proved in Appendix B.2) *Given a target task \mathcal{T} with N_0 i.i.d. samples generated from 1-dimensional underlying model $P_{X;\theta_0}$, and a source task \mathcal{S}_1 with N_1 i.i.d. samples generated from 1-dimensional underlying model $P_{X;\theta_1}$, where $\theta_0, \theta_1 \in \mathbb{R}$. $\hat{\theta}$ is denoted as the MLE (4) based on the N_0 samples from \mathcal{T} and n_1 samples from \mathcal{S}_1 , where $n_1 \in [0, N_1]$, then the K-L measure (6) can be expressed as:*

$$\frac{1}{2} \left(\underbrace{\frac{1}{N_0 + n_1}}_{\text{variance term}} + \underbrace{\frac{n_1^2}{(N_0 + n_1)^2 t}}_{\text{bias term}} \right) + o\left(\frac{1}{N_0 + n_1}\right), \quad (8)$$

where

$$t \triangleq J(\theta_0)(\theta_1 - \theta_0)^2. \quad (9)$$

Moreover, the optimal transfer quantity n_1^* is

$$n_1^* = \begin{cases} N_1, & \text{if } N_0 \cdot t \leq 0.5 \\ \min\left(N_1, \frac{N_0}{2N_0 t - 1}\right), & \text{if } N_0 \cdot t > 0.5 \end{cases}. \quad (10)$$

From (8), we observe that the K-L measure decreases as N_0 increases, which aligns with our intuition that utilizing all available target samples is beneficial. In addition, the trend of (8) with respect to n_1 is more complex. We plot (8) as a function of n_1 under two different regimes, determined by the value of $N_0 \cdot t$, as shown in Figure 2. Our goal is to explore the optimal value of n_1^* to minimize (8).

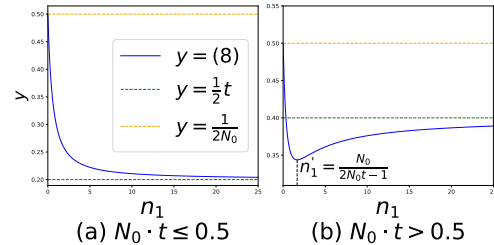


Figure 2: The function curve figures of (8) under different regimes determined by the value of $N_0 \cdot t$ (blue). The vertical axis denotes the value of K-L measure (8), while the horizontal axis denotes the variable n_1 .

- **Case 1** ($N_0 \cdot t \leq 0.5$): The K-L measure monotonically decreases as n_1 increases. Obviously, the optimal point is $n_1^* = N_1$. This indicates that when the source task and the target task are highly similar, i.e., when t is small, an increase in the transfer quantity will positively impact the results.
- **Case 2** ($N_0 \cdot t > 0.5$): The K-L measure first decreases and then increases as n_1 increases. It attaining its minimum at $n_1' = \frac{N_0}{2N_0 t - 1}$. It should be noted that

when t is large enough, the point n_1' approaches 0. This aligns with the intuition that when the discrepancy between the source and target tasks is substantial, avoiding transfer yields better results. Furthermore, if n_1' exceeds N_1 , we should utilize all N_1 samples, so $n_1^* = \min\left(N_1, \frac{N_0}{2N_0t-1}\right)$.

In Figure 3, we provide an intuitive explanation for the optimal n_1^* .

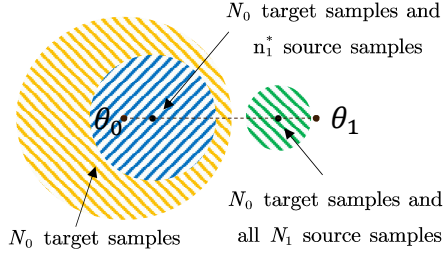


Figure 3: The three circles represent the errors corresponding to transfer quantity $n_1 = 0$, n_1^* , and N_1 . The distance from each circle's center to θ_0 represents the bias of estimation, and the radius represents the variance. As the transfer quantity increases, the bias increases, while the variance decreases. The optimal n_1^* achieves the best trade-off between them.

As the dimensionality of the model parameter θ increases to higher dimensions, we derive the following propositions.

Proposition 4.4. (proved in Appendix B.3) *In the case where the parameter dimension is d , i.e., $\underline{\theta}_0 \in \mathbb{R}^d$, with all other settings remaining the same as the Lemma 4.2, the K-L measure (6) can be expressed as*

$$\frac{d}{2N_0} + o\left(\frac{1}{N_0}\right). \quad (11)$$

Proposition 4.5. (proved in Appendix B.4) *In the case where the parameter dimension is d , i.e., $\underline{\theta}_0, \underline{\theta}_1 \in \mathbb{R}^d$, with all other settings remaining the same as the Theorem 4.3, the K-L measure (6) can be expressed as*

$$\frac{d}{2} \left(\frac{1}{N_0 + n_1} + \frac{n_1^2}{(N_0 + n_1)^2} t \right) + o\left(\frac{1}{N_0 + n_1}\right), \quad (12)$$

where we denote

$$t \triangleq \frac{(\underline{\theta}_1 - \underline{\theta}_0)^T J(\underline{\theta}_0) (\underline{\theta}_1 - \underline{\theta}_0)}{d}. \quad (13)$$

In addition, t is a scalar, $J(\underline{\theta}_0)$ is $d \times d$ matrix, and $(\underline{\theta}_1 - \underline{\theta}_0)$ is a d -dimensional vector, which is the element-wise subtraction of two d -dimensional vectors $\underline{\theta}_1$ and $\underline{\theta}_0$.

Compared to Theorem 4.3, Proposition 4.5 exhibits a similar mathematical form, allowing us to derive the optimal transfer quantity through a similar approach. Furthermore, we observe that as the parameter dimension d increases, the K-L error measure (12) increases. This suggests that for a complex model, knowledge transfer across tasks becomes more challenging, which is consistent with the findings in (Tong et al., 2021).

4.2. Multi-Source Transfer Learning

Consider the multi-source transfer learning scenario with K source task $\{\mathcal{S}_1, \dots, \mathcal{S}_K\}$ and one target task \mathcal{T} . We aim to derive the optimal transfer quantity n_i^* of each source.

Theorem 4.6. (proved in Appendix B.5) *Given a target task \mathcal{T} with N_0 i.i.d. samples generated from underlying model $P_{X;\underline{\theta}_0}$, and K source tasks $\mathcal{S}_1, \dots, \mathcal{S}_K$ with N_1, \dots, N_K i.i.d. samples generated from underlying model $P_{X;\underline{\theta}_1}, \dots, P_{X;\underline{\theta}_K}$, where $\underline{\theta}_0, \underline{\theta}_1, \dots, \underline{\theta}_K \in \mathbb{R}^d$. $\hat{\underline{\theta}}$ is denoted as the MLE (4) based on the N_0 samples from \mathcal{T} and n_1, \dots, n_K samples from $\mathcal{S}_1, \dots, \mathcal{S}_K$, where $n_i \in [0, N_i]$. Denoting $\tilde{s} = \sum_{i=1}^K n_i$ as the total transfer quantity, and $\alpha_i = \frac{n_i}{\tilde{s}}$ as the proportion of different source tasks, then the K-L measure (6) can be expressed as:*

$$\frac{d}{2} \left(\frac{1}{N_0 + \tilde{s}} + \frac{\tilde{s}^2}{(N_0 + \tilde{s})^2} t \right) + o\left(\frac{1}{N_0 + \tilde{s}}\right). \quad (14)$$

In (14), t is a scalar denoted as

$$t = \frac{\underline{\alpha}^T \Theta^T J(\underline{\theta}_0) \Theta \underline{\alpha}}{d}, \quad (15)$$

where $\underline{\alpha} = [\alpha_1, \dots, \alpha_K]^T$ is a K -dimensional vector, and $\Theta^{d \times K} = [\underline{\theta}_1 - \underline{\theta}_0, \dots, \underline{\theta}_K - \underline{\theta}_0]$.

According to Theorem 4.6, we can derive the optimal transfer quantities n_1^*, \dots, n_K^* by minimizing (14). Equivalently, we need to find the optimal total transfer quantity s^* and the optimal proportion vector $\underline{\alpha}^*$ which minimize (14). The analytical solutions of s^* and $\underline{\alpha}^*$ are difficult to acquire, and we provide a method to get their numerical solutions in Appendix D. Eventually, we can get the optimal transfer quantity of each source through $n_i^* = s^* \cdot \alpha_i^*$.

4.3. Practical Algorithm

Along with our theoretical framework, we propose a practical algorithm, OTQMS, which is applicable to all supervised target tasks, as presented in Algorithm 1. It mainly involves two stages: (1) initializing the source task parameters $\theta_1, \dots, \theta_K$ to compute the optimal transfer quantities and (2) jointly training the target model using a resampled dataset whose sample quantity of each source corresponds to the optimal transfer quantity derived from our theory.

Table 2: **Multi-Source Transfer Performance on DomainNet and Office-Home.** The arrows indicate transferring from the rest tasks. The highest/second-highest accuracy is marked in Bold/Underscore form respectively.

Method	Backbone	DomainNet							Office-Home				
		→C	→I	→P	→Q	→R	→S	Avg	→Ar	→Cl	→Pr	→Rw	Avg
Unsupervised-all-shots													
MSFDA(Shen et al., 2023)	ResNet50	66.5	21.6	56.7	20.4	70.5	54.4	48.4	75.6	62.8	84.8	<u>85.3</u>	77.1
DATE(Han et al., 2023)	ResNet50	-	-	-	-	-	-	-	75.2	60.9	85.2	84.0	76.3
M3SDA(Peng et al., 2019)	ResNet101	57.2	24.2	51.6	5.2	61.6	49.6	41.5	-	-	-	-	-
Supervised-10-shots													
<i>Few-Shot Methods:</i>													
H-ensemble(Wu et al., 2024)	ViT-S	53.4	21.3	54.4	19.0	70.4	44.0	43.8	71.8	47.5	77.6	79.1	69.0
MADA(Zhang et al., 2024)	ViT-S	51.0	12.8	60.3	15.0	81.4	22.7	40.5	78.4	58.3	82.3	85.2	76.1
MADA(Zhang et al., 2024)	ResNet50	66.1	23.9	<u>60.4</u>	<u>31.9</u>	<u>75.4</u>	52.5	51.7	72.2	<u>64.4</u>	82.9	81.9	75.4
MCW(Lee et al., 2019)	ViT-S	54.9	21.0	53.6	20.4	70.8	42.4	43.9	68.9	48.0	77.4	86.0	70.1
WADN(Shui et al., 2021)	ViT-S	68.0	29.7	59.1	16.8	74.2	55.1	50.5	60.3	39.7	66.2	68.7	58.7
<i>Source-Ablation Methods:</i>													
Target-Only	ViT-S	14.2	3.3	23.2	7.2	41.4	10.6	16.7	40.0	33.3	54.9	52.6	45.2
Single-Source-Avg	ViT-S	50.4	22.1	44.9	24.7	58.8	42.5	40.6	65.2	53.3	74.4	72.7	66.4
Single-Source-Best	ViT-S	60.2	28.0	55.4	28.4	66.0	49.7	48.0	72.9	60.9	80.7	74.8	72.3
AllSources \cup Target	ViT-S	<u>71.7</u>	<u>32.4</u>	60.0	31.4	71.7	<u>58.5</u>	<u>54.3</u>	77.0	62.3	84.9	84.5	<u>77.2</u>
OTQMS (Ours)	ViT-S	72.8	33.8	61.2	33.8	73.2	59.8	55.8	<u>78.1</u>	64.5	85.2	84.9	78.2

Algorithm 1 OTQMS: Training

- 1: **Input:** Target data $D_{\mathcal{T}} = \{(z_{\mathcal{T}}^i, y_{\mathcal{T}}^i)\}_{i=1}^{N_0}$, source data $\{D_{S_k} = \{(z_{S_k}^i, y_{S_k}^i)\}_{i=1}^{N_k}\}_{k=1}^K$, model type f_{θ} and its parameters θ_0 for target task and $\{\theta_k\}_{k=1}^K$ for source tasks, parameter dimension d .
// z represents the feature and y represents the label
- 2: **Parameter:** Learning rate η .
- 3: **Initialize:** randomly initialize $\theta_0, \{\theta_k\}_{k=1}^K$.
- 4: **Output:** a well-trained model f_{θ_0} for target task.
- 5: **for** $k = 1$ **to** K **do** // Initialize the source parameters
- 6: **repeat**
- 7: $L_k \leftarrow \frac{1}{N_k} \sum_{i=1}^{N_k} \ell(y_{S_k}^i, f_{\theta_k}(z_{S_k}^i))$
- 8: $\theta_k \leftarrow \theta_k - \eta \nabla_{\theta_k} L_k$
- 9: **until** θ_k converges;
- 10: **end for**
- 11: **repeat** // Joint training of the target task
- 12: $L_{\mathcal{T}} \leftarrow \frac{1}{N_{train}} \sum_{i=1}^{N_{train}} \ell(y_{\mathcal{T}}^i, f_{\theta_0}(z^i))$
- 13: $\theta_0 \leftarrow \theta_0 - \eta \nabla_{\theta_0} L_{\mathcal{T}}$
- 14: $\Theta \leftarrow [\theta_1 - \theta_0, \dots, \theta_K - \theta_0]^T$
- 15: $J(\theta_0) \leftarrow (\nabla_{\theta_0} L_{\mathcal{T}})(\nabla_{\theta_0} L_{\mathcal{T}})^T$
- 16: $(s^*, \underline{\alpha}^*) \leftarrow \arg \min_{(s, \underline{\alpha})} \frac{d}{2} \left(\frac{1}{N_0+s} + \frac{s^2}{(N_0+s)^2} \frac{\alpha^T \Theta^T J(\theta_0) \Theta \alpha}{d} \right)$
- 17: $D_{source} \leftarrow \bigcup_{k=1}^K \left\{ D_{S_k}^* \mid D_{S_k}^* \subseteq D_{S_k}, |D_{S_k}^*| = s^* \alpha_k^* \right\}$
- 18: $D_{train} \leftarrow D_{source} \cup D_{\mathcal{T}}$
- 19: **until** θ_0 converges;

5. Experiments**5.1. Experiments Settings**

Benchmark Datasets. DomainNet contains 586,575 samples of 345 classes from 6 domains (*i.e.*, **C**: Clipart, **I**: Infograph, **P**: Painting, **Q**: Quickdraw, **R**: Real and **S**: Sketch). Office-Home benchmark contains 15588 samples of 65 classes, with 12 adaptation scenarios constructed from 4 domains: Art, Clipart, Product and Real World (abbr. **Ar**, **Cl**, **Pr** and **Rw**). Digits contains four-digit sub-datasets: MNIST(mt), Synthetic(sy), SVHN(sv) and USPS(up), with each sub-dataset containing samples of numbers ranging from 0 to 9.

Implementation Details. We employ the ViT-Small model (Wightman, 2019), pre-trained on ImageNet-21k (Deng et al., 2009), as the backbone for all datasets. The Adam optimizer is employed with a learning rate of $1e^{-5}$. We allocate 20% of the dataset as the test set, and report the highest accuracies within 5 epoch early stops in all experiments. Following the standard few-shot learning protocol, the training data for k-shot consists of k randomly selected samples per class from the target task. All experiments are conducted on Nvidia A800 GPUs.

Baselines. For a general performance evaluation, we take SOTA works under similar settings as baselines. The scope of compared methods includes: 1) Unsupervised Methods: MSFDA (Shen et al., 2023), DATE (Han et al., 2023), M3SDA (Peng et al., 2019). 2) Few-Shot Methods Based on Model(Parameter)-Weighting: H-ensemble (Wu et al., 2024), MCW (Lee et al., 2019). 3) Few-Shot Methods Based on Sample: MADA (Zhang et al., 2024), WADN (Shui

et al., 2021) 4) Source Ablating Methods: Target-Only, Single-Source-Avg/Single-Source-Best (average/best performance of single-source transfer), AllSources \cup Target (all source & target data in multi-source transfer). Note that MADA (Zhang et al., 2024) leverages all unlabeled target data in conjunction with a limited amount of labeled target data, which is a hybrid approach combining unsupervised and supervised learning. Due to the page limit, we provide detailed information on the experimental design and the results of an experiment adapted to the WADN settings on the Digits dataset in Appendix C.2.

5.2. Main Result

We evaluated our algorithm, OTQMS, alongside baseline methods on the multi-source transfer learning tasks using the DomainNet and Office-Home datasets. The quantitative results are summarized in Table 2. Since the unsupervised baselines are not designed for the supervised few-shot setting, we report their original results from the respective papers for reference. We make the following observations:

Overall Performance. In general, compared to baseline methods, OTQMS achieves the best performance on almost all the transfer scenarios on the two datasets. Specifically, OTQMS outperforms the state-of-the-art (AllSources \cup Target) by an average of 1.5% on DomainNet and 1.0% on Office-Home.

Data Speaks Louder Than Model Weighting. It is worth noting that on both datasets, samples-based methods utilizing both target and source samples to jointly train the model, such as WADN, MADA and OTQMS, generally outperform model(parameter)-weighting approaches which construct the target model by weighting source models, such as H-ensemble and MCW. This observation suggests that sample-based approaches offer greater advantages over model-based methods, because they can fully leverage the relevant information from the source data for the target task.

Take, But Only as Much as You Need. Comparing results in Table 2 among Target-only, AllSources \cup Target, and OTQMS, we observe that OTQMS achieves the best performance in both datasets by leveraging only a subset of data selected from all available sources based on model preference. This result validates our theory and highlights the benefits of identifying the optimal balance in the bias-variance trade-off. By choosing the right quantities of samples from the source tasks, we could train the target model more accurately. Furthermore, Figure 5 shows that OTQMS also significantly reduces the training time and sample usage, which validates its superiority in terms of data efficiency.

Few-Shot Labels, Big Gains. We make a comparison of the results of unsupervised and supervised methods. While other conditions remain the same, Table 2 demonstrates

that even if unsupervised methods like MSFDA and M3SDA take all the target data into account (up to 1.3×10^5 samples on Real domain of DomainNet), their performance still falls short compared to the supervised methods, which rely on only a limited number of samples (3450 samples). This illustrates the importance of having supervised information in multi-source transfer learning.

5.3. Static vs. Dynamic Transfer Quantity

In our proposed Algorithm 1, we employ a ‘‘Dynamic’’ strategy that dynamically determines the optimal transfer quantities and updates the resampled dataset during the joint training of target task. To validate the effectiveness of this strategy, we conducted comparative experiments using the ‘‘Static-’’ methods. ‘‘Static-’’ methods first simulate the distribution of target on target dataset only, and different types of Static such as ‘‘Under, Exact and Over’’ stands for different fitting levels. In ‘‘Static-’’ methods, we only compute the optimal transfer quantity once to make the resampled dataset, and evaluated on it until target model converges. The results on Table 3 demonstrate OTQMS using dynamic transfer quantity achieved the best performance.

Table 3: Static vs. Dynamic Transfer Quantity in OTQMS on Office-Home. Arrows will transfer from the rest tasks.

Method	Backbone	Office-Home				
		\rightarrow Ar	\rightarrow Cl	\rightarrow Pr	\rightarrow Rw	Avg
<i>Supervised-10-shots:</i>						
Static-Under	ViT-S	<u>77.0</u>	<u>62.3</u>	84.9	<u>84.5</u>	<u>77.2</u>
Static-Exact	ViT-S	46.0	59.8	<u>85.1</u>	83.7	68.7
Static-Over	ViT-S	76.8	61.9	<u>78.6</u>	68.6	71.5
Dynamic	ViT-S	78.1	64.5	85.2	84.9	78.2

5.4. Generality across Different Shot Settings

As discussed in the theoretical analysis of Theorem 4.3, our theoretical framework is applicable to any quantity of target samples. Therefore, OTQMS exhibits shot generality, enabling it to avoid negative transfer across different shot settings. To validate this, we increase the number of shots from 5 to 100 across methods including AllSources \cup Target, Target-Only, and OTQMS. As shown in Figure 4, experimental results demonstrate that OTQMS consistently outperforms other approaches across all shot settings. This highlights the generality and scalability of OTQMS in terms of data utilization.

5.5. Data Efficiency Test

In this section, we demonstrate the advantage of OTQMS in terms of data efficiency. Specifically, we conduct experiments with MADA, AllSources \cup Target, and OTQMS across different shot settings, and for each shot setting, we

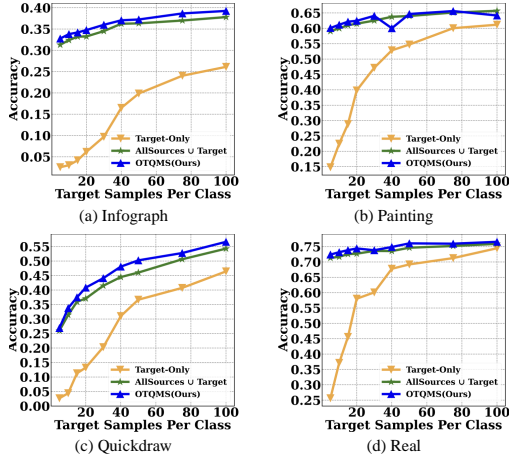


Figure 4: Performance comparison with increasing target shots up to 100 per class on DomainNet dataset (I, P, Q and R domains). OTQMS (blue) outperforms other methods.

accumulate the total sample used and time consumed until the highest accuracy is reached. To better visualize the results, we present the average sample usage and training time across all shot settings in Figure 5. To be specific, OTQMS reduces the average training time by 35.19% and the average sample usage by 47.85% on DomainNet, compared to the AllSources \cup Target method.

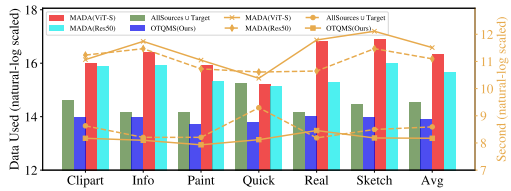


Figure 5: Data efficiency comparison of average sample usage and training time on DomainNet dataset, the left vertical axis represents the amount of sample usage, with green bars indicating AllSources \cup Target data counts, blue bars about OTQMS, red bars about MADA(ViT-S) and azury bars about MADA(Res50), while the right orange vertical axis and lines represent training time.

5.6. Compatibility to Parameter-Efficient Training

To evaluate the applicability with parameter-efficient training, we used a ViT-Base model (Dosovitskiy et al., 2021) integrated with the LoRA framework (Hu et al., 2021) as the backbone. This approach significantly reduces the number of trainable parameters for downstream tasks while ensuring model quality and improving training efficiency. In the experiments, we consider the trainable low-rank matrices and the classification head as the parametric model in our theoretical framework, while treating the remaining parameters as constants. Other experimental settings are the same as de-

fault. Experiments were conducted on the Office-Home dataset. The results of Table 5 in Appendix demonstrate that our method remains effective.

5.7. Analysis on Domain-specific Transfer Quantity

To understand the domain preference of OTQMS, we visualize the proportion of each source in the selected samples for each target domain. As shown in Figure 6(b), when the target domain is Clipart, OTQMS primarily leverages samples from Real, Painting, and Sketch. In addition, Quickdraw contributes minimally to any target domain. These observations align with the findings in (Peng et al., 2019). To further clarify the selection process of OTQMS during training, we visualize it in Figure 6(a). We observe that in the Office-Home dataset, Clipart initially selects all source domains but later focuses on Art and Real World. In the DomainNet dataset, Sketch predominantly selects Clipart, Painting, and Real throughout the training process.

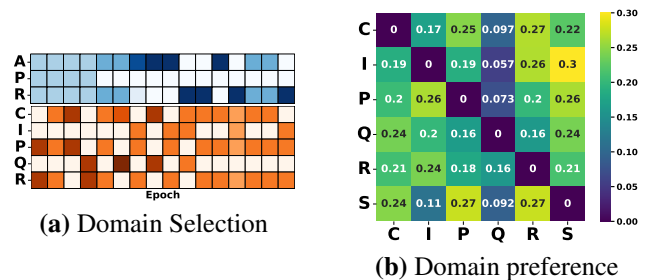


Figure 6: Visualization of domain-specific transfer quantity under 10-shot setting. (a) Domain selection during training epochs (from left to right), where the blue upper part represents the selection of target domain Clipart on Office-Home, and the orange lower part represents the selection of target domain Sketch on DomainNet. Darker colors indicate stronger tendencies throughout the training process. (b) Source domain preferences of different target domains on DomainNet. Each row corresponds to a target domain while each column represents a source domain.

6. Conclusion

In this work, we propose a theoretical framework to determine the optimal transfer quantities in multi-source transfer learning. Our framework reveals that by optimizing the transfer quantity of each source task, we can improve target task training while reducing the total transfer quantity. Based on this theoretical framework, we develop an architecture-agnostic and data-efficient practical algorithm OTQMS for jointly training the target model. We evaluated the proposed algorithm through extensive experiments and demonstrated its superior accuracy and enhanced data efficiency.

Impact Statement

This paper presents work whose goal is to advance the field of Machine Learning. There are many potential societal consequences of our work, none which we feel must be specifically highlighted here.

References

- Bao, Y., Li, Y., Huang, S.-L., Zhang, L., Zheng, L., Zamir, A., and Guibas, L. An information-theoretic approach to transferability in task transfer learning. In *2019 IEEE international conference on image processing (ICIP)*, pp. 2309–2313. IEEE, 2019.
- Bu, Y., Zou, S., and Veeravalli, V. V. Tightening mutual information-based bounds on generalization error. *IEEE Journal on Selected Areas in Information Theory*, 1(1): 121–130, 2020.
- Courty, N., Flamary, R., Tuia, D., and Rakotomamonjy, A. Optimal transport for domain adaptation. *IEEE transactions on pattern analysis and machine intelligence*, 39(9): 1853–1865, 2016.
- Cover, T. and Thomas, J. A. Elements of information theory, 2006.
- Deng, J., Dong, W., Socher, R., Li, L.-J., Li, K., and Fei-Fei, L. Imagenet: A large-scale hierarchical image database. In *2009 IEEE conference on computer vision and pattern recognition*, pp. 248–255. Ieee, 2009.
- Dosovitskiy, A., Beyer, L., Kolesnikov, A., Weissenborn, D., Zhai, X., Unterthiner, T., Dehghani, M., Minderer, M., Heigold, G., Gelly, S., Uszkoreit, J., and Houshy, N. An image is worth 16x16 words: Transformers for image recognition at scale. *ICLR*, 2021.
- Fu, J., Yuan, F., Song, Y., Yuan, Z., Cheng, M., Cheng, S., Zhang, J., Wang, J., and Pan, Y. Exploring adapter-based transfer learning for recommender systems: Empirical studies and practical insights. In *Proceedings of the 17th ACM International Conference on Web Search and Data Mining*, pp. 208–217, 2024.
- Guo, H., Pasunuru, R., and Bansal, M. Multi-source domain adaptation for text classification via distancenet-bandits. In *Proceedings of the AAAI conference on artificial intelligence*, volume 34, pp. 7830–7838, 2020.
- Han, Z., Zhang, Z., Wang, F., He, R., Su, W., Xi, X., and Yin, Y. Discriminability and transferability estimation: a bayesian source importance estimation approach for multi-source-free domain adaptation. In *Proceedings of the AAAI Conference on Artificial Intelligence*, volume 37, pp. 7811–7820, 2023.
- Harremoës, P. and Vajda, I. On pairs of f -divergences and their joint range. *IEEE Transactions on Information Theory*, 57(6):3230–3235, 2011.
- Hu, E. J., Shen, Y., Wallis, P., Allen-Zhu, Z., Li, Y., Wang, S., Wang, L., and Chen, W. Lora: Low-rank adaptation of large language models. *arXiv preprint arXiv:2106.09685*, 2021.
- Langley, P. Crafting papers on machine learning. In Langley, P. (ed.), *Proceedings of the 17th International Conference on Machine Learning (ICML 2000)*, pp. 1207–1216, Stanford, CA, 2000. Morgan Kaufmann.
- Lee, J., Sattigeri, P., and Wornell, G. Learning new tricks from old dogs: Multi-source transfer learning from pre-trained networks. *Advances in neural information processing systems*, 32, 2019.
- Li, K., Lu, J., Zuo, H., and Zhang, G. Multi-source contribution learning for domain adaptation. *IEEE Transactions on Neural Networks and Learning Systems*, 33(10):5293–5307, 2021a.
- Li, Y., Yuan, L., Chen, Y., Wang, P., and Vasconcelos, N. Dynamic transfer for multi-source domain adaptation. In *Proceedings of the IEEE/CVF Conference on Computer Vision and Pattern Recognition*, pp. 10998–11007, 2021b.
- Long, M., Wang, J., Ding, G., Sun, J., and Yu, P. S. Transfer joint matching for unsupervised domain adaptation. In *Proceedings of the IEEE conference on computer vision and pattern recognition*, pp. 1410–1417, 2014.
- Nguyen, C., Hassner, T., Seeger, M., and Archambeau, C. Leep: A new measure to evaluate transferability of learned representations. In *International Conference on Machine Learning*, pp. 7294–7305. PMLR, 2020.
- Peng, X., Bai, Q., Xia, X., Huang, Z., Saenko, K., and Wang, B. Moment matching for multi-source domain adaptation. In *Proceedings of the IEEE/CVF international conference on computer vision*, pp. 1406–1415, 2019.
- Shen, M., Bu, Y., and Wornell, G. W. On balancing bias and variance in unsupervised multi-source-free domain adaptation. In *International Conference on Machine Learning*, pp. 30976–30991. PMLR, 2023.
- Shui, C., Li, Z., Li, J., Gagné, C., Ling, C. X., and Wang, B. Aggregating from multiple target-shifted sources. In *International Conference on Machine Learning*, pp. 9638–9648. PMLR, 2021.
- Sun, S., Shi, H., and Wu, Y. A survey of multi-source domain adaptation. *Information Fusion*, 24:84–92, 2015.

- Sung, Y.-L., Cho, J., and Bansal, M. VI-adapter: Parameter-efficient transfer learning for vision-and-language tasks. In *Proceedings of the IEEE/CVF conference on computer vision and pattern recognition*, pp. 5227–5237, 2022.
- Tong, X., Xu, X., Huang, S.-L., and Zheng, L. A mathematical framework for quantifying transferability in multi-source transfer learning. *Advances in Neural Information Processing Systems*, 34:26103–26116, 2021.
- Vincent, V., Wannes, M., and Jesse, D. Transfer learning for anomaly detection through localized and unsupervised instance selection. In *Proceedings of the AAAI Conference on Artificial Intelligence*, volume 34, pp. 6054–6061, 2020.
- Wan, L., Liu, R., Sun, L., Nie, H., and Wang, X. Uav swarm based radar signal sorting via multi-source data fusion: A deep transfer learning framework. *Information Fusion*, 78:90–101, 2022.
- Wang, M. and Deng, W. Deep visual domain adaptation: A survey. *Neurocomputing*, 312:135–153, 2018.
- Wightman, R. Pytorch image models. <https://github.com/huggingface/pytorch-image-models>, 2019.
- Wu, Y., Wang, J., Wang, W., and Li, Y. H-ensemble: An information theoretic approach to reliable few-shot multi-source-free transfer. In *Proceedings of the AAAI Conference on Artificial Intelligence*, volume 38, pp. 15970–15978, 2024.
- Zhang, W., Lv, Z., Zhou, H., Liu, J.-W., Li, J., Li, M., Li, Y., Zhang, D., Zhuang, Y., and Tang, S. Revisiting the domain shift and sample uncertainty in multi-source active domain transfer. In *Proceedings of the IEEE/CVF Conference on Computer Vision and Pattern Recognition*, pp. 16751–16761, 2024.
- Zhao, S., Yue, X., Zhang, S., Li, B., Zhao, H., Wu, B., Krishna, R., Gonzalez, J. E., Sangiovanni-Vincentelli, A. L., Seshia, S. A., et al. A review of single-source deep unsupervised visual domain adaptation. *IEEE Transactions on Neural Networks and Learning Systems*, 33(2):473–493, 2020.
- Zhao, S., Li, B., Xu, P., Yue, X., Ding, G., and Keutzer, K. Madan: Multi-source adversarial domain aggregation network for domain adaptation. *International Journal of Computer Vision*, 129(8):2399–2424, 2021.
- Zhao, S., Chen, H., Huang, H., Xu, P., and Ding, G. More is better: Deep domain adaptation with multiple sources. *arXiv preprint arXiv:2405.00749*, 2024.
- Zhuang, F., Qi, Z., Duan, K., Xi, D., Zhu, Y., Zhu, H., Xiong, H., and He, Q. A comprehensive survey on transfer learning. *Proceedings of the IEEE*, 109(1):43–76, 2020.

A. Notations

Symbol	Description
\mathcal{T}	target task
$\{\mathcal{S}_1, \dots, \mathcal{S}_K\}$	source tasks
N_0	quantity of target samples
$N_1 \dots N_k$	maximum sample quantity of each source
$n_1 \dots n_k$	transfer quantity of each source
θ	model parameter
$\underline{\theta}$	vectorized model parameter
$\underline{\theta}_0$	vectorized model parameter of target task
$\underline{\theta}_i, i \in [1, K]$	vectorized model parameter of i-th source task,
$J(\theta)$	Fisher information (scalar) of θ
$J(\underline{\theta})^{d \times d}$	Fisher information (matrix) of d-dimensional $\underline{\theta}$
$P(X; \theta)$	probability of X parameterized by θ
$P_{X; \theta}$	distribution of X parameterized by θ
$\ \underline{x}\ ^2$	l-2 norm of vector x
α_i	transfer proportion in multi-source case from i-th source task
$\underline{\alpha}$	transfer proportion vector in multi-source case whose i-th entry is α_i
s	total transfer quantity in multi-source case
$\hat{\theta}$	estimator of θ
$E_{\hat{\theta}}$	expectation of $\hat{\theta}$

Table 4: Notations

B. Proofs

B.1. Proof of Lemma 4.2

Lemma B.1. *In the asymptotic case, the K-L measure (6) and the mean squared error have the relation as follows.*

$$\begin{aligned} & \mathbb{E} \left[D \left(P_{X;\hat{\theta}} \parallel P_{X;\theta_0} \right) \right] \\ &= \frac{1}{2} J(\theta_0) \text{MSE}(\hat{\theta}) + o\left(\frac{1}{N_0}\right), \end{aligned} \quad (16)$$

Proof. In this section, for the sake of clarity, we will write $\hat{\theta}$ in its parameterized form $\hat{\theta}(X^{N_0})$ when necessary, and these two forms are mathematically equivalent. By taking Taylor expansion of $D \left(P_{X;\hat{\theta}(X^{N_0})} \parallel P_{X;\theta_0} \right)$ at θ_0 , we can get

$$D \left(P_{X;\hat{\theta}(X^{N_0})} \parallel P_{X;\theta_0} \right) = \frac{1}{2} \sum_{x \in X} \frac{\left(P_{X;\hat{\theta}(X^{N_0})}(x) - P_{X;\theta_0}(x) \right)^2}{P_{X;\theta_0}(x)} + o(\|\hat{\theta}(X^{N_0}) - \theta_0\|^2) \quad (17)$$

We denote δ as a small constant, and we can rewrite (6) as

$$\begin{aligned} & \mathbb{E} \left[D \left(P_{X;\hat{\theta}(X^{N_0})} \parallel P_{X;\theta_0} \right) \right] \\ &= \sum_{X^{N_0}} P_{X^n;\theta_0}(X^{N_0}) D \left(P_{X;\hat{\theta}(X^{N_0})} \parallel P_{X;\theta_0} \right) \\ &= \sum_{X^{N_0}} P_{X^n;\theta_0}(X^{N_0}) \left(\frac{1}{2} \sum_{x \in X} \frac{\left(P_{X;\hat{\theta}(X^{N_0})}(x) - P_{X;\theta_0}(x) \right)^2}{P_{X;\theta_0}(x)} + o(\|\hat{\theta}(X^{N_0}) - \theta_0\|^2) \right) \\ &= \sum_{X^{N_0}} P_{X^n;\theta_0}(X^{N_0}) \left(\frac{1}{2} \sum_{x \in X} \frac{\left(\frac{\partial P_{X;\theta_0}(x)}{\partial \theta_0} (\hat{\theta}(X^{N_0}) - \theta_0) \right)^2}{P_{X;\theta_0}(x)} + o(\|\hat{\theta}(X^{N_0}) - \theta_0\|^2) \right) \\ &= \sum_{\{X^{N_0}; \|\hat{\theta}(X^{N_0}) - \theta_0\|^2 < \delta\}} P_{X^n;\theta_0}(X^{N_0}) \left(\frac{1}{2} \sum_{x \in X} \frac{\left(\frac{\partial P_{X;\theta_0}(x)}{\partial \theta_0} (\hat{\theta}(X^{N_0}) - \theta_0) \right)^2}{P_{X;\theta_0}(x)} + o(\|\hat{\theta}(X^{N_0}) - \theta_0\|^2) \right) \\ &+ \sum_{\{X^{N_0}; \|\hat{\theta}(X^{N_0}) - \theta_0\|^2 \geq \delta\}} P_{X^n;\theta_0}(X^{N_0}) \left(\frac{1}{2} \sum_{x \in X} \frac{\left(\frac{\partial P_{X;\theta_0}(x)}{\partial \theta_0} (\hat{\theta}(X^{N_0}) - \theta_0) \right)^2}{P_{X;\theta_0}(x)} + o(\|\hat{\theta}(X^{N_0}) - \theta_0\|^2) \right) \end{aligned} \quad (18)$$

To facilitate the subsequent proof, we introduce the concept of "Dot Equal".

Definition B.2. (Dot Equal (\doteq)) Specifically, given two functions $f(n)$ and $g(n)$, the notation $f(n) \doteq g(n)$ is defined as

$$f(n) \doteq g(n) \Leftrightarrow \lim_{n \rightarrow \infty} \frac{1}{n} \log \frac{f(n)}{g(n)} = 0, \quad (19)$$

which shows that $f(n)$ and $g(n)$ have the same exponential decaying rate.

We denote $\hat{P}_{X^{N_0}}$ as the empirical distribution of X^{N_0} . Applying Sanov's Theorem to (18), we can know that

$$P_{X^n;\theta_0}(X^{N_0}) \doteq e^{-N_0 D(\hat{P}_{X^{N_0}} \parallel P_{X;\theta_0})} \quad (20)$$

Then, we aim to establish a connection between the K-L divergence (20) and $\|\hat{\theta}(X^{N_0}) - \theta_0\|^2$. From (17), we can know that

$$D\left(\hat{P}_{X^{N_0}} \parallel P_{X;\theta_0}\right) = \frac{1}{2} \sum_{x \in X} \frac{\left(\hat{P}_{X^{N_0}}(x) - P_{X;\theta_0}(x)\right)^2}{P_{X;\theta_0}(x)} + o(\|\hat{\theta}(X^{N_0}) - \theta_0\|^2) \quad (21)$$

From the features of MLE, we can know that

$$\mathbb{E}_{\hat{P}_{X^{N_0}}} \left[\frac{\partial \log P_{X;\hat{\theta}(X^{N_0})}(x)}{\partial \hat{\theta}} \right] = 0 = \mathbb{E}_{\hat{P}_{X^{N_0}}} \left[\frac{\partial \log P_{X;\theta_0}(x)}{\partial \theta_0} \right] + \mathbb{E}_{\hat{P}_{X^{N_0}}} \left[\frac{\partial^2 \log P_{X;\theta_0}(x)}{\partial \theta_0^2} \right] \left(\hat{\theta}(X^{N_0}) - \theta_0 \right), \quad (22)$$

which can be transform to

$$\left(\hat{\theta}(X^{N_0}) - \theta_0 \right) = \frac{\mathbb{E}_{\hat{P}_{X^{N_0}}} \left[\frac{\partial \log P_{X;\theta_0}(x)}{\partial \theta_0} \right]}{\mathbb{E}_{\hat{P}_{X^{N_0}}} \left[\frac{\partial^2 \log P_{X;\theta_0}(x)}{\partial \theta_0^2} \right]} = \frac{\mathbb{E}_{\hat{P}_{X^{N_0}}} \left[\frac{\frac{\partial P_{X;\theta_0}(x)}{\partial \theta_0}}{P_{X;\theta_0}(x)} \right]}{\mathbb{E}_{\hat{P}_{X^{N_0}}} \left[\frac{\partial^2 \log P_{X;\theta_0}(x)}{\partial \theta_0^2} \right]} = \frac{\sum_{x \in X} \left(\hat{P}_{X^{N_0}}(x) - P_{X;\theta_0}(x) \right) \frac{\frac{\partial P_{X;\theta_0}(x)}{\partial \theta_0}}{P_{X;\theta_0}(x)}}{J(\theta_0)} \quad (23)$$

Using the Cauchy-Schwarz inequality, we can obtain

$$\sum_{x \in X} \frac{\left(\hat{P}_{X^{N_0}}(x) - P_{X;\theta_0}(x) \right)^2}{P_{X;\theta_0}(x)} \cdot \sum_x \frac{\left(\frac{\partial P_{X;\theta_0}(x)}{\partial \theta_0} \right)^2}{P_{X;\theta_0}(x)} \geq \left(\sum_{x \in X} \left(\hat{P}_{X^{N_0}}(x) - P_{X;\theta_0}(x) \right) \frac{\frac{\partial P_{X;\theta_0}(x)}{\partial \theta_0}}{P_{X;\theta_0}(x)} \right)^2 \quad (24)$$

where

$$\sum_x \frac{\left(\frac{\partial P_{X;\theta_0}(x)}{\partial \theta_0} \right)^2}{P_{X;\theta_0}(x)} = \sum_x P_{X;\theta_0}(x) \left(\frac{1}{P_{X;\theta_0}(x)} \frac{\partial P_{X;\theta_0}(x)}{\partial \theta_0} \right)^2 = \sum_x P_{X;\theta_0}(x) \left(\frac{\partial \log P_{X;\theta_0}(x)}{\partial \theta_0} \right)^2 = J(\theta_0) \quad (25)$$

Combining with (21), (23), and (25), the inequality (24) can be transformed to

$$D\left(\hat{P}_{X^{N_0}} \parallel P_{X;\theta_0}\right) \geq \frac{J(\theta_0) \left(\hat{\theta}(X^{N_0}) - \theta_0 \right)^2}{2} = \frac{J(\theta_0) \|\hat{\theta}(X^{N_0}) - \theta_0\|^2}{2} \quad (26)$$

Combining (20) and (26), we can know that

$$P_{X^n;\theta_0}(X^{N_0}) \doteq e^{-N_0 D(\hat{P}_{X^{N_0}} \parallel P_{X;\theta_0})} \leq e^{-\frac{N_0 J(\theta_0) \|\hat{\theta}(X^{N_0}) - \theta_0\|^2}{2}} \quad (27)$$

For the first term in (18), the $\|\hat{\theta}(X^{N_0}) - \theta_0\|$ is small enough for us to omit the term $o(\|\hat{\theta}(X^{N_0}) - \theta_0\|^2)$. As for the second term in (18), even though the magnitude of $\|\hat{\theta}(X^{N_0}) - \theta_0\|$ is no longer negligible, the probability of such sequences is $O(e^{-\frac{N_0 J(\theta_0) \|\hat{\theta}(X^{N_0}) - \theta_0\|^2}{2}})$ by (27), which is exponentially decaying with N_0 such that the second term is $o(\frac{1}{N_0})$. By transferring (18), we can get

$$\begin{aligned} & \mathbb{E} \left[D\left(P_{X;\hat{\theta}(X^{N_0})} \parallel P_{X;\theta_0}\right) \right] \\ &= \sum_{\{X^{N_0} : \|\hat{\theta}(X^{N_0}) - \theta_0\|^2 < \delta\}} P_{X^n;\theta_0}(X^{N_0}) \left(\frac{1}{2} \sum_{x \in X} \frac{\left(\frac{\partial P_{X;\theta_0}(x)}{\partial \theta_0} (\hat{\theta}(X^{N_0}) - \theta_0) \right)^2}{P_{X;\theta_0}(x)} \right) + o(\|\hat{\theta}(X^{N_0}) - \theta_0\|^2) \\ &+ \sum_{\{X^{N_0} : \|\hat{\theta}(X^{N_0}) - \theta_0\|^2 \geq \delta\}} P_{X^n;\theta_0}(X^{N_0}) \left(\frac{1}{2} \sum_{x \in X} \frac{\left(\frac{\partial P_{X;\theta_0}(x)}{\partial \theta_0} (\hat{\theta}(X^{N_0}) - \theta_0) \right)^2}{P_{X;\theta_0}(x)} \right) + o\left(\frac{1}{N_0}\right) \\ &= \frac{1}{2} \mathbb{E} \left[\frac{1}{2} \sum_{x \in X} \frac{\left(\frac{\partial P_{X;\theta_0}(x)}{\partial \theta_0} (\hat{\theta}(X^{N_0}) - \theta_0) \right)^2}{P_{X;\theta_0}(x)} \right] + o\left(\frac{1}{N_0}\right). \end{aligned} \quad (28)$$

We then transform (28) with (25)

$$\begin{aligned}
 & \frac{1}{2} \mathbb{E} \left[\sum_{x \in X} \frac{\left(\frac{\partial P_{X; \theta_0}(x)}{\partial \theta_0} (\hat{\theta}(X^{N_0}) - \theta_0) \right)^2}{P_{X; \theta_0}(x)} \right] \\
 &= \frac{1}{2} \mathbb{E} \left[(\hat{\theta} - \theta_0)^2 \sum_x \frac{\left(\frac{\partial P_{X; \theta_0}(x)}{\partial \theta_0} \right)^2}{P_{X; \theta_0}(x)} \right] \\
 &= \frac{1}{2} \mathbb{E} \left[(\hat{\theta} - \theta_0)^2 \right] J(\theta_0)
 \end{aligned} \tag{29}$$

Combining (28), (29), we can get

$$\mathbb{E} \left[D \left(P_{X; \hat{\theta}} \parallel P_{X; \theta_0} \right) \right] = \frac{1}{2} \mathbb{E} \left[(\hat{\theta} - \theta_0)^2 \right] J(\theta_0) + o\left(\frac{1}{N_0}\right). \tag{30}$$

□

From (16), we can establish the relationship between the proposed K-L measure (6) and the mean squared error. Then, by using the (3), the K-L measure is

$$\frac{1}{2N_0} + o\left(\frac{1}{N_0}\right). \tag{31}$$

B.2. Proof of Theorem 4.3

In this section we will be using samples from both distributions for our maximum likelihood estimation, so our optimization problem becomes

$$\hat{\theta} = \arg \max_{\theta} L_n(\theta), \tag{32}$$

where, when using N_0 samples from target task, and n_1 samples from source task

$$L_n(\theta) \triangleq \frac{1}{N_0 + n_1} \sum_{x \in X^{N_0}} \log P_{X; \theta}(x) + \frac{1}{N_0 + n_1} \sum_{x \in X^{n_1}} \log P_{X; \theta}(x). \tag{33}$$

And, we also define the expectation of our estimator, which is somewhere between θ_0 and θ_1 to be $E_{\hat{\theta}}$

$$E_{\hat{\theta}} = \arg \max_{\theta} L(\theta), \tag{34}$$

We could equivalently transform (34) into

$$E_{\hat{\theta}} = \arg \min_{\theta} \frac{N_0 D(P_{X; \theta_0} \parallel P_{X; \theta})}{N_0 + n_1} + \frac{n_1 D(P_{X; \theta_1} \parallel P_{X; \theta})}{N_0 + n_1} \tag{35}$$

By taking argmin of (35) we can get

$$P_{X; E_{\hat{\theta}}} = \frac{N_0 P_{X; \theta_0} + n_1 P_{X; \theta_1}}{N_0 + n_1}, \tag{36}$$

By doing a Taylor Expansion of (36) around θ' , which is in the neighbourhood of θ_1, θ_2 and $E_{\hat{\theta}}$, we can get

$$E_{\hat{\theta}} = \frac{N_0 \theta_0 + n_1 \theta_1}{N_0 + n_1} + O\left(\frac{1}{N_0 + n_1}\right), \tag{37}$$

Lemma B.3.

$$\sqrt{N_0 + n_1}(\hat{\theta} - E_{\hat{\theta}}) \xrightarrow{d} \mathcal{N}\left(0, \frac{1}{J(\theta_0)}\right) \quad (38)$$

Proof. Since $\hat{\theta}$ is a maximizer of $L_n(\theta)$, $L'_n(\hat{\theta}) = 0 = L'_n(E_{\hat{\theta}}) + L''_n(E_{\hat{\theta}})(\hat{\theta} - E_{\hat{\theta}})$. Therefore,

$$\sqrt{N_0 + n_1}(\hat{\theta} - E_{\hat{\theta}}) = \frac{\sqrt{N_0 + n_1}L'_n(E_{\hat{\theta}})}{L''_n(E_{\hat{\theta}})}. \quad (39)$$

Since $E_{\hat{\theta}}$ maximizes $L(\theta)$, $L'(E_{\hat{\theta}}) = \frac{N_0}{N_0 + n_1}\mathbb{E}_{\theta_0}\left[\frac{\partial \log P_{X;E_{\hat{\theta}}}(x)}{\partial x}\right] + \frac{n_1}{N_0 + n_1}\mathbb{E}_{\theta_1}\left[\frac{\partial \log P_{X;E_{\hat{\theta}}}(x'_i)}{\partial x}\right] = 0$. Therefore,

$$\begin{aligned} & \sqrt{N_0 + n_1}L'_n(E_{\hat{\theta}}) \\ &= \sqrt{\frac{N_0}{N_0 + n_1}}\left(\sqrt{\frac{1}{N_0}}\sum_{x \in X^{N_0}}\frac{\partial \log P_{X;E_{\hat{\theta}}}(x)}{\partial \theta} - \sqrt{N_0}\mathbb{E}_{\theta_0}\left[\frac{\partial \log P_{X;E_{\hat{\theta}}}(x)}{\partial \theta}\right]\right) \\ &+ \sqrt{\frac{n_1}{N_0 + n_1}}\left(\sqrt{\frac{1}{n_1}}\sum_{x \in X^{n_1}}\frac{\partial \log P_{X;E_{\hat{\theta}}}(x)}{\partial \theta} - \sqrt{n_1}\mathbb{E}_{\theta_1}\left[\frac{\partial \log P_{X;E_{\hat{\theta}}}(x)}{\partial \theta}\right]\right) \end{aligned} \quad (40)$$

Applying the Central Limit Theorem to (40), we can get

$$\begin{aligned} \sqrt{N_0 + n_1}L'_n(E_{\hat{\theta}}) &\xrightarrow{a.s.} \mathcal{N}\left(0, \frac{N_0}{N_0 + n_1}\left(\mathbb{E}_{\theta_0}\left[\left(\frac{\partial \log P_{X;E_{\hat{\theta}}}(x)}{\partial \theta}\right)^2\right] - \mathbb{E}_{\theta_0}\left[\left(\frac{\partial \log P_{X;E_{\hat{\theta}}}(x)}{\partial \theta}\right)\right]^2\right) + \right. \\ &\quad \left. \frac{n_1}{N_0 + n_1}\left(\mathbb{E}_{\theta_1}\left[\left(\frac{\partial \log P_{X;E_{\hat{\theta}}}(x)}{\partial \theta}\right)^2\right] - \mathbb{E}_{\theta_1}\left[\left(\frac{\partial \log P_{X;E_{\hat{\theta}}}(x)}{\partial \theta}\right)\right]^2\right)\right) \end{aligned} \quad (41)$$

By taking Taylor expansion of $E_{\hat{\theta}}$ at θ_1 , we can get

$$\begin{aligned} & \mathbb{E}_{\theta_0}\left[\left(\frac{\partial \log P_{X;E_{\hat{\theta}}}(x)}{\partial \theta}\right)^2\right] \\ &= \mathbb{E}_{\theta_0}\left[\left(\frac{\partial \log P_{X;\theta_0}(x)}{\partial \theta} + \frac{\partial}{\partial \theta}\frac{\partial \log P_{X;\theta_0}(x)}{\partial \theta}(E_{\hat{\theta}} - \theta_0) + O\left(\frac{1}{N_0 + n_1}\right)\right)^2\right] \\ &= J(\theta_0) + (E_{\hat{\theta}} - \theta_0)\mathbb{E}_{\theta_0}\left[\frac{\partial \log P_{X;E_{\hat{\theta}}}(x)}{\partial \theta}\frac{\partial^2 \log P_{X;E_{\hat{\theta}}}(x)}{\partial \theta^2}\right] + O\left(\frac{1}{N_0 + n_1}\right) \\ &= J(\theta_0) + O\left(\frac{1}{\sqrt{N_0 + n_1}}\right) \end{aligned} \quad (42)$$

and

$$\begin{aligned} & \mathbb{E}_{\theta_0}\left[\left(\frac{\partial \log P_{X;E_{\hat{\theta}}}(x)}{\partial \theta}\right)^2\right] \\ &= \mathbb{E}_{\theta_0}\left[\left(\frac{\partial \log P_{X;\theta_0}(x)}{\partial \theta} + \frac{\partial}{\partial \theta}\frac{\partial \log P_{X;\theta_0}(x)}{\partial \theta}(E_{\hat{\theta}} - \theta_0) + O\left(\frac{1}{N_0 + n_1}\right)\right)^2\right] \\ &= \mathbb{E}_{\theta_0}\left[\left(\frac{\partial}{\partial \theta}\frac{\partial \log P_{X;\theta_0}(x)}{\partial \theta}(E_{\hat{\theta}} - \theta_0) + O\left(\frac{1}{N_0 + n_1}\right)\right)^2\right] \\ &= (E_{\hat{\theta}} - \theta_0)^2\mathbb{E}_{\theta_0}\left[\left(\frac{\partial}{\partial \theta}\frac{\partial \log P_{X;\theta_0}(x)}{\partial \theta}\right)^2\right] + o\left(\frac{1}{N_0 + n_1}\right) \\ &= O\left(\frac{1}{N_0 + n_1}\right) \end{aligned} \quad (43)$$

By combining (41), (42), and (43), we can get

$$\text{var} \left(\sqrt{N_0 + n_1} L'_n(E_{\hat{\theta}}) \right) = \frac{N_0}{N_0 + n_1} J(\theta_0) + \frac{n_1}{N_0 + n_1} J(\theta_1) + O\left(\frac{1}{\sqrt{N_0 + n_1}}\right) \quad (44)$$

Additionally, we know $L''_n(E_{\hat{\theta}}) \xrightarrow{P} J(E_{\hat{\theta}})$. Combining with (39)(44), we know that

$$\sqrt{N_0 + n_1}(\hat{\theta} - E_{\hat{\theta}}) \xrightarrow{d} \mathcal{N} \left(0, \frac{\frac{N_0}{N_0+n_1} J(\theta_0) + \frac{n_1}{N_0+n_1} J(\theta_1)}{J^2(E_{\hat{\theta}})} \right) \quad (45)$$

Under the assumption that $\theta_0, \theta_1, E_{\hat{\theta}}$ are sufficiently close to each other, we can easily deduce that the difference among $J(\theta_0), J(\theta_1)$ and $J(E_{\hat{\theta}})$ is $O(\frac{1}{\sqrt{N_0+n_1}})$. We can easily get

$$\sqrt{N_0 + n_1}(\hat{\theta} - E_{\hat{\theta}}) \xrightarrow{d} \mathcal{N} \left(0, \frac{1}{J(\theta_0)} \right) \quad (46)$$

□

Therefore, the bound of $\mathbb{E} \left[(\hat{\theta} - E_{\hat{\theta}})^2 \right]$ is

$$\frac{1}{(N_0 + n_1)J(\theta_0)} \quad (47)$$

Combining (6) and (29), we know that

$$\begin{aligned} & \mathbb{E} \left[D \left(P_{X;\hat{\theta}} \parallel P_{X;\theta_0} \right) \right] \\ &= \frac{1}{2} J(\theta_0) \mathbb{E} \left[(\hat{\theta} - \theta_0)^2 \right] + o\left(\frac{1}{N_0}\right) \\ &= \frac{1}{2} J(\theta_0) \left(\mathbb{E} \left[(\hat{\theta} - E_{\hat{\theta}})^2 \right] + \mathbb{E} \left[2(\hat{\theta} - E_{\hat{\theta}})(E_{\hat{\theta}} - \theta_0) \right] + \mathbb{E} \left[(E_{\hat{\theta}} - \theta_0)^2 \right] \right) + o\left(\frac{1}{N_0}\right) \\ &= \frac{1}{2} J(\theta_0) \left(\mathbb{E} \left[(\hat{\theta} - E_{\hat{\theta}})^2 \right] + \mathbb{E} \left[(E_{\hat{\theta}} - \theta_0)^2 \right] \right) + o\left(\frac{1}{N_0}\right) \end{aligned} \quad (48)$$

Combining (48), (37) and (47), we know that the K-L measure is

$$\frac{1}{2} \frac{1}{N_0 + n_1} + \frac{1}{2} J(\theta_0) \frac{n_1^2}{(N_0 + n_1)^2} (\theta_1 - \theta_0)^2 \quad (49)$$

B.3. Proof of Proposition 4.4

Similar to (16), we can get

$$\begin{aligned} & \mathbb{E} \left[D \left(P_{X;\hat{\theta}} \parallel P_{X;\underline{\theta}_0} \right) \right] \\ &= \frac{1}{2} \text{tr} \left(J(\underline{\theta}_0) \mathbb{E} \left[(\hat{\underline{\theta}} - \underline{\theta}_0) (\hat{\underline{\theta}} - \underline{\theta}_0)^T \right] \right) + o\left(\frac{1}{N_0}\right) \end{aligned} \quad (50)$$

Combining with Lemma 3.1, we will know that the K-L measure is

$$\frac{1}{2} \text{tr} \left(J(\underline{\theta}_0) \left(J(\underline{\theta}_0)^{-1} \frac{1}{N_0} + o\left(\frac{1}{N_0}\right) \right) \right) = \frac{d}{2N_0} + o\left(\frac{1}{N_0}\right) \quad (51)$$

B.4. Proof of Proposition 4.5

Similar to (48), we can get

$$\begin{aligned}
 & \mathbb{E} \left[D \left(P_{X;\hat{\theta}} \middle| P_{X;\theta_0} \right) \right] \\
 &= \frac{1}{2} \text{tr} \left(J(\theta_0) \mathbb{E} \left[\left(\hat{\theta} - \theta_0 \right) \left(\hat{\theta} - \theta_0 \right)^T \right] \right) + o\left(\frac{1}{N_0}\right) \\
 &= \frac{1}{2} \left(\text{tr} \left(J(\theta_0) \mathbb{E} \left[\left(\hat{\theta} - E_{\hat{\theta}} \right) \left(\hat{\theta} - E_{\hat{\theta}} \right)^T \right] \right) + \text{tr} \left(J(\theta_0) \mathbb{E} \left[\left(E_{\hat{\theta}} - \theta_0 \right) \left(E_{\hat{\theta}} - \theta_0 \right)^T \right] \right) \right) + o\left(\frac{1}{N_0}\right) \quad (52)
 \end{aligned}$$

Similar to (38), we can get

$$\sqrt{N_0 + n_1} \left(\hat{\theta} - E_{\hat{\theta}} \right) \xrightarrow{d} \mathcal{N} \left(0, J(\theta_0)^{-1} \right) \quad (53)$$

So we can know that $\mathbb{E} \left[\left(\hat{\theta} - E_{\hat{\theta}} \right)^2 \right]$ has the bound

$$\frac{1}{(N_0 + n_1)} J(\theta_0)^{-1} \quad (54)$$

The same to (37), we can get

$$E_{\hat{\theta}} = \frac{N_0 \theta_0 + n_1 \theta_1}{N_0 + n_1} + O \left(\frac{1}{N_0 + n_1} \right), \quad (55)$$

Combining (52), (54) and (55), we can know that the K-L measure is

$$\frac{d}{2} \left(\frac{1}{N_0 + n_1} + \frac{n_1^2}{(N_0 + n_1)^2} t \right) + o \left(\frac{1}{N_0 + n_1} \right), \quad (56)$$

where we denote

$$t \triangleq \frac{(\theta_1 - \theta_0)^T J(\theta_0) (\theta_1 - \theta_0)}{d}. \quad (57)$$

B.5. Proof of Theorem 4.6

Proof. Similar to (38), we can get

$$\sqrt{N_0 + \sum_{i=1}^K n_i} \left(\hat{\theta} - E_{\hat{\theta}} \right) \xrightarrow{d} \mathcal{N} \left(0, J(\theta_0)^{-1} \right) \quad (58)$$

So we can know that $\mathbb{E} \left[\left(\hat{\theta} - E_{\hat{\theta}} \right)^2 \right]$ has the bound

$$\frac{1}{(N_0 + s)} J(\theta_0)^{-1} \quad (59)$$

Similar to (37), we can get

$$E_{\hat{\theta}} = \frac{N_0 \theta_0 + \sum_{i=1}^k n_i \theta_i}{N_0 + \sum_{i=1}^K n_i} = \frac{N_0 \theta_0 + \sum_{i=1}^k n_i \theta_i}{N_0 + s} + O \left(\frac{1}{N_0 + s} \right) \quad (60)$$

Combining (48), (59) and (60), we can know that the K-L measure is

$$\frac{1}{2} \frac{1}{N_0 + s} + \frac{1}{2} \frac{s^2}{(N_0 + s)^2} J(\underline{\theta}_0) \left(\sum_{i=1}^k \alpha_i (\underline{\theta}_i - \underline{\theta}_0) \right)^2 + o\left(\frac{1}{N_0 + s}\right) \quad (61)$$

For the d-dimension parameter, we can know that the K-L measure is θ_i

$$\begin{aligned} & \frac{d}{2} \left(\frac{1}{N_0 + s} + \frac{s^2}{(N_0 + s)^2 d} \text{tr} \left(\mathbf{J}(\underline{\theta}_0) \left(\sum_{i=1}^k \alpha_i (\underline{\theta}_i - \underline{\theta}_0) \right) \left(\sum_{i=1}^k \alpha_i (\underline{\theta}_i - \underline{\theta}_0) \right)^T \right) \right) \\ &= \frac{d}{2} \left(\frac{1}{N_0 + s} + \frac{s^2}{(N_0 + s)^2} \frac{\underline{\alpha}^T \Theta^T \mathbf{J}(\underline{\theta}_0) \Theta \underline{\alpha}}{d} \right) + o\left(\frac{1}{N_0 + s}\right) \end{aligned} \quad (62)$$

where $\underline{\alpha} = [\alpha_1, \dots, \alpha_K]^T$ is a K-dimensional vector, and

$$\Theta^{d \times K} = [\underline{\theta}_1 - \underline{\theta}_0, \dots, \underline{\theta}_K - \underline{\theta}_0]. \quad (63)$$

□

C. Experiment Details

C.1. Details information of LoRA framework experiments.

Table 5: Multi-Source Transfer with LoRA on Office-Home. We apply LoRA on ViT-B backbone for PEFT.

Method	Backbone	Office-Home				
		→Ar	→Cl	→Pr	→Rw	Avg
<i>Supervised-10-shots Source-Ablation:</i>						
Target-Only	ViT-B	59.8	42.2	69.5	72.0	60.9
Single-Source-avg	ViT-B	72.2	59.9	82.6	81.0	73.9
Single-Source-best	ViT-B	74.4	61.8	84.9	81.9	75.8
AllSources \cup Target	ViT-B	<u>81.1</u>	<u>66.0</u>	<u>88.0</u>	<u>89.2</u>	<u>81.1</u>
OTQMS (Ours)	ViT-B	81.5	68.0	89.2	90.3	82.3

C.2. Experimental Design and Model Adaptation

To ensure consistency in the experimental setup, we first evaluate the performance of different methods on the DomainNet and Office-Home datasets by adapting their settings to align with ours, such as the backbone, dataset, and early stopping criteria. Specifically, for the MADA method, we adjusted the preset of keeping 5% of labeled target samples to 10-shots per class target samples while maintaining other conditions. And in turn, ours is adapted to the WADN settings, equipped with a 3-layer ConvNet and evaluated on Digits dataset.

Table 6: **Performance on Digits Dataset.** The arrows indicate transferring from the rest tasks. “3Conv” denotes the backbone with 3 convolution layers.

Method	Backbone	Digits				
		→mt	→sv	→sy	→up Avg	
<i>Following settings of WADN:</i>						
WADN(Shui et al., 2021)	3Conv	88.3	70.6	81.5	90.5	82.7
AllSources \cup Target	3Conv	<u>92.6</u>	<u>67.1</u>	<u>82.5</u>	88.8	<u>82.8</u>
OTQMS (Ours)	3Conv	93.8	<u>67.1</u>	83.3	<u>89.1</u>	83.3

C.3. Single-Source transfer performance details.

Table 7: **Single-Source Transfer Performance on DomainNet.** The details accuracy information of the “Single-Source-*” lines of Table 2.

Target Domain	Backbone	Source Domain							
		Clipart	Infograph	Painting	Quickdraw	Real	Sketch	Avg	Best
Clipart	ViT-S	-	46.5	55.4	30.3	60.2	59.7	50.4	60.2
Infograph	ViT-S	25.6	-	25.3	7.3	28.0	24.4	22.1	28.0
Painting	ViT-S	49.6	47.3	-	22.4	55.4	49.6	44.9	55.4
Quickdraw	ViT-S	26.9	18.1	23.9	-	25.9	28.4	24.7	28.4
Real	ViT-S	64.6	62.2	66.0	38.5	-	62.7	58.8	66.0
Sketch	ViT-S	49.7	40.9	48.1	26.1	47.8	-	42.5	49.7

Table 8: **Single-Source Transfer Performance on Office-Home.** The details accuracy information of the “Single-Source-*” lines of Table 2.

Target Domain	Backbone	Source Domain					
		Art	Clipart	Product	Real World	Avg	Best
Art	ViT-S	-	61.7	61.1	72.9	65.2	72.9
Clipart	ViT-S	49.8	-	49.4	60.9	53.3	60.9
Product	ViT-S	68.8	73.7	-	80.7	74.4	80.7
Real World	ViT-S	70.9	72.3	74.8	-	72.7	74.8

Table 9: **Single-Source Transfer Performance on Office-Home of LoRA.** The details accuracy information of the “Single-Source-*” lines of Table 5. ViT-B backbone is already frozen and equipped with small trainable LoRA layers.

Target Domain	Backbone	Source Domain					
		Art	Clipart	Product	Real World	Avg	Best
Art	ViT-B	-	68.4	74.4	73.8	72.2	74.4
Clipart	ViT-B	58.3	-	59.6	61.8	59.9	61.8
Product	ViT-B	82.0	80.8	-	84.9	82.6	84.9
Real World	ViT-B	81.0	80.3	81.9	-	81.0	81.9

C.4. Baselines experiments settings in Table 2.

Since the significant difference from unsupervised methods and supervised methods, the results of MSFDA(Shen et al., 2023), DATE(Han et al., 2023) and M3SDA(Peng et al., 2019) are directly supported by their own article.

On all the experiments of the baselines, we take all the source samples of different domains from trainset into account. And types of the backbone are all pretrained on ImageNet21k(Deng et al., 2009).

As for based on model-parameter-weighting few-shot methods: MCW(Lee et al., 2019) and H-ensemble(Wu et al., 2024), since they have not taken experiments on DomainNet and Office-Home datasets with ViT-Small backbone and 10-shot per class training samples, we take it by changing the backbone and samples condition while maintaining other configurations supported by their own work. And for fairness and efficiency, the well-trained source models from different domains of these methods are directly equipped with the same models trained by the first stage of our OTQMS method respectively.

As for based on samples few-shot methods: We exam the WADN(Shui et al., 2021) method under the condition of limited label on target domain as this setting is similar to ours. And we also change the backbone and samples condition while maintaining other configurations of its report to realize the experiments on DomainNet and Office-Home datasets. It is apparent that the settings of MADA(Zhang et al., 2024) are quite different of ours, leveraging all the labeled source data and all the unlabeled target data with the few-shot labeled ones that are difficult to classify, which means all the target samples have been learned to some extent. So we not only decrease the labeled target samples to 10-shot per class but also the unlabeled target samples. And since MADA is the most SOTA and comparable method, we realize it with our fair

10-shot setting under both ViT-S and ResNet50 backbone on DomainNet and Office-Home datasets while maintaining other configurations of its report.

C.5. Data efficient test details in 5.5 .

Table 10: **Data Efficient Test Results on DomainNet.** The capital letters represent the target domains.

Method	Backbone	Data Counts ($\times 10^6$)							Training Consumed Time ($\times 10^4$ Second)						
		C	I	P	Q	R	S	Avg	C	I	P	Q	R	S	Avg
MADA(Zhang et al., 2024)	ViT-S	8.70	13.39	8.31	4.02	19.76	21.32	12.58	6.40	12.52	6.29	3.22	13.19	18.18	9.97
MADA(Zhang et al., 2024)	ResNet50	7.83	8.21	4.57	3.69	4.35	8.78	6.24	7.56	9.58	4.56	4.05	4.21	9.58	6.59
AllSources \cup Target	ViT-S	2.17	1.42	1.42	4.20	1.42	1.90	2.09	0.56	0.37	0.39	1.09	0.36	0.49	0.54
OTQMS (Ours)	ViT-S	1.18	1.15	0.89	0.97	1.19	1.16	1.09	0.35	0.33	0.28	0.34	0.47	0.36	0.35

Table 11: **Data Efficient Log Scaled Test Results on DomainNet.** The capital letters represent the target domains.

Method	Backbone	Data Counts (log scale)							Training Consumed Time (log scale)						
		C	I	P	Q	R	S	Avg	C	I	P	Q	R	S	Avg
MADA(Zhang et al., 2024)	ViT-S	15.98	16.41	15.93	15.21	16.80	16.87	16.35	11.07	11.74	11.05	10.38	11.79	12.11	11.51
MADA(Zhang et al., 2024)	ResNet50	15.87	15.92	15.33	15.12	15.29	15.99	15.65	11.23	11.47	10.73	10.61	10.65	11.47	11.10
AllSources \cup Target	ViT-S	14.59	14.17	14.18	15.25	14.17	14.46	14.55	8.63	8.21	8.21	9.30	8.19	8.50	8.59
OTQMS (Ours)	ViT-S	13.98	13.95	13.70	13.78	13.99	13.96	13.90	8.17	8.10	7.93	8.12	8.46	8.18	8.17

C.6. Domain choosing analysis details.

To compute the heatmap matrix visualizing domain preference in Figure 6(b), for each source domain, we count the samples selected from it until the target model converges under the 10-shot condition. Since the quantities of available samples varies significantly across domains, we normalize the counts by these quantities. The final domain preference is then determined by computing the importance of these normalized values.

Similarly, to compute the heatmap matrix for domain selection in Figure 6(a), we calculate the importance of the counts of selected samples from different source domains throughout the training epochs.

D. Method to get s^* and $\underline{\alpha}^*$ which minimize (14) in Theorem 4.6

The minimization problem of K-L measure (14) is

$$(s^*, \underline{\alpha}^*) \leftarrow \arg \min_{(s, \underline{\alpha})} \frac{d}{2} \left(\frac{1}{N_0 + s} + \frac{s^2}{(N_0 + s)^2} \frac{\underline{\alpha}^T \Theta^T J(\underline{\theta}_0) \Theta \underline{\alpha}}{d} \right). \quad (64)$$

We decompose this problem and explicitly formulate the constraints as follows.

$$(s^*, \underline{\alpha}^*) \leftarrow \arg \min_{s \in [0, \sum_{i=1}^K N_i]} \frac{d}{2} \left(\frac{1}{N_0 + s} + \frac{s^2}{(N_0 + s)^2 d} \arg \min_{\underline{\alpha} \in \mathcal{A}(s)} \underline{\alpha}^T \Theta^T J(\underline{\theta}_0) \Theta \underline{\alpha} \right), \quad (65)$$

where

$$\mathcal{A}(s) = \left\{ \underline{\alpha} \mid \sum_{i=1}^K \alpha_i = 1, s * \alpha_i \leq N_i, \alpha_i \geq 0, i = 1, \dots, K \right\}. \quad (66)$$

Due to the complex constraints between s and α , obtaining an analytical solution to this problem is challenging. Therefore, we propose a numerical approach to get the optimal solution. Specifically, we perform a grid search over the feasible domain of s . For each candidate s' , we compute the optimal α' under the constraint $\mathcal{A}(s')$, which is a $K \times K$ quadratic programming problem with respect to α . The K-L measure (14) value is then evaluated using (s', α') . After completing the search over s , the optimal values s^* and α^* correspond to the pair (s', α') that minimizes the K-L measure.